www.lajss.org
Latin American Journal of Solids and Structures 2 (2005) 77–88

Strong displacement discontinuities and Lagrange multipliers: finite displacement formulation in the analysis of fracture problems

P. M. A. Areias, J. M. A. César de Sá[a,*] and C. A. Conceição António

IDMEC – Instituto de Engenharia Mecânica
FEUP – Faculdade de Engenharia da Universidade do Porto, Portugal

Abstract

A finite displacement formulation of a quadrilateral element containing an embedded displacement discontinuity is presented. Lagrange multipliers are adopted to ensure the crack closure before initiation. Six additional degrees of freedom in each element allow the representation of the various states of the crack. The discretized equilibrium equations are exposed, along with the corresponding exact linearization. Two examples illustrate both the robustness and the accuracy of the algorithms.

Keywords: Embedded discontinuities, fracture, finite displacement, Lagrangre multipliers.

1 Introduction

The modern finite element analysis of crack initiation and propagation in solids can be carried out through the use of embedded strong discontinuities.

Studies regarding embedded strong discontinuities were carried out, for example, in references [2, 5, 6, 8, 9] for small strain situations and in reference [7] for finite strain situations using triangular elements. These techniques circumvent the necessity for remeshing and require less parameters than standard regularized strain softening implementations. However, penalty parameters are often adopted for closing the crack.

The use of Lagrange multipliers for closing the crack before propagation is clearly an appropriate methodology to avoid penalty parameters and therefore reduce the amount of data required to accomplish a simulation.

Two important aspects for an efficient implicit finite element analysis of these problems are the algorithm robustness and the verified rate of convergence of the Newton-Raphson method (which, for conservative systems with Lagrange multipliers, can be classified as Lagrange-Newton). Here, an exact linearization of the discretized equilibrium equations is carried out.

* Corresponding author E-mail: cesarsa@fe.up.pt
Received 05 November 2004
From *Recent Developments in the Modelling of Rupture in Solids Conference*, ed. A. Benallal & S.P.B. Proença.

2 The kinematics of the element

2.1 The element with an embedded displacement discontinuity: notation

For conciseness, the general considerations regarding the presence of a displacement discontinuity can be consulted elsewhere (see references [2, 9]).

A study of the quadrilateral element resented in Figure 1 is carried out.

The crack mid-line is identified through the vector OP and the crack position is identified by the point O. It is noticeable that, if finite displacements are considered, it may occur that the two crack faces can be widely separated.

Two local director vectors corresponding to a local frame are also represented, which can be obtained from the vector OP: S is the tangential vector and N is the normal vector.

The proposed element with embedded discontinuity contains 4 nodes ($k = 1, 2, 3, 4$), as illustrated in Figure 1. This figure also presents three sets of points Ω_1 and Ω_2 (such as $\Omega_1 \cap \Omega_2 = \emptyset$) and Γ. This last set of points represents the crack.

The complete element as a set of points is identify as Ω, such that $\Omega = \Omega_1 \cup \Omega_2 \cup \Gamma$ with $\Omega_1 \cap \Gamma = \emptyset$ and $\Omega_2 \cap \Gamma = \emptyset$.

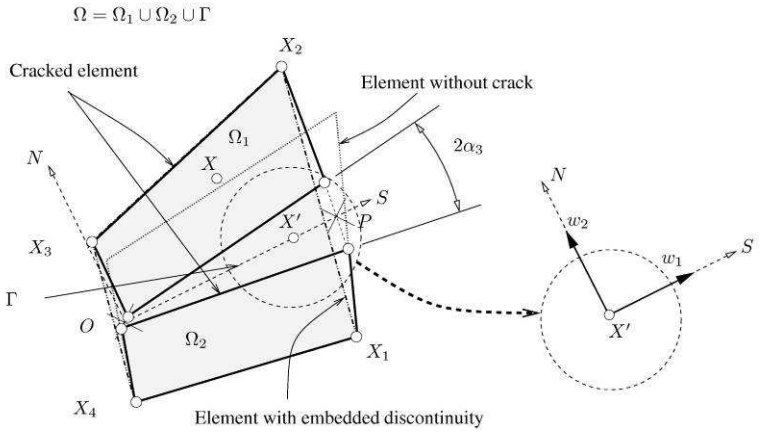

Figure 1: The representation of the embedded discontinuity for a single quadrilateral element (OP identifies the crack mid-line). A configuration with crack opening is shown.

In the presently adopted notation, a given point is denoted as X, its material and spatial positions are denoted as $\boldsymbol{X}$ and $\boldsymbol{x}$ respectively. A converged position of X is identified as $\boldsymbol{X}^*$. Finally the i^{th} scalar component of $\boldsymbol{X}$ is presented as X_i.

2.2 Rigid body motion result from the crack

The existence of a crack, Γ, which separates the two parts of the element, Ω_1 and Ω_2 (see Figure 1) induces rigid body motions in these two parts.

The rigid body motion displacements field of the two separated elements parts (Ω_1 and Ω_2 in 1) should be included into the original displacement field corresponding to the non-cracked element.

If the converge coordinates $\boldsymbol{X}^*$ of an arbitrary point $X \in \Omega_1 \cup \Omega_2$ are considered, the displacement vector of this point due to the crack induced rigid body motion can be approximately calculated as:

$$\bar{u}\left(X^*, \mathrm{r}\right) = \begin{bmatrix} S_1^* & N_1^* \\ S_2^* & N_2^* \end{bmatrix} \left\{ \left(\underbrace{\begin{bmatrix} \cos\alpha_3 & -r\,sen\alpha_3 \\ r\,sen\alpha_3 & \cos\alpha_3 \end{bmatrix} \begin{bmatrix} O^*X^*.S^* \\ O^*X^*.N^* \end{bmatrix} - \begin{bmatrix} O^*X^*.S^* \\ O^*X^*.N^* \end{bmatrix}}_{rotation} \right) + \underbrace{\begin{bmatrix} r\,\alpha_1 \\ r\,\alpha_2 \end{bmatrix}}_{displacement} \right\} \tag{1}$$

where α_1, α_2, α_3 are internal variables and r is a number belonging to the set $\{-1, 1\}$.

This definition presents the use of three internal variables α_i. The variable α_3 represents the crack face rotation. The variables α_1 and α_2 represent the local displacements of the upper crack face at the point O (see Figure 1).

These internal variables are additive, in contrast with the result $\bar{u}$.

A representation of the scalar components of $\bar{u}$ can be carried out as $\bar{u}_1 = f_1\left(\alpha_1, \alpha_2, \alpha_3\right)$ and $\bar{u}_2 = f_2\left(\alpha_1, \alpha_2, \alpha_3\right)$. The functions f_1 e f_2 are introduced to allow the representation of the displacement jump at Γ.

The motivation of the use of the parameter $r \in \{-1, 1\}$ in equation (1) is to identify the set of points to which X belongs. For $X \in \Omega_1$ then $r = 1$ and for $X \in \Omega_2$ then $r = -1$.

For the analysis of the crack opening, it is necessary to rewrite a relation analogous to (1) in local coordinates and valid for $X \in \Gamma$.

In the local frame S, N the scalar components of the local relative displacements at Γ can be denoted as w_1 and w_2. To ensure that no penetration takes place between Ω_1 and Ω_2 it is necessary to verify $w_1 \in \Re$ and $w_2 \in \Re_0^+$.

The global displacement $\bar{w}$ corresponding to the local coordinates w_1 and w_2 can be written as:

$$\bar{w} = \begin{bmatrix} S_1^* & N_1^* \\ S_2^* & N_2^* \end{bmatrix} \begin{bmatrix} w_1 \\ w_2 \end{bmatrix} \quad in\ \Gamma \tag{2}$$

If the crack is closed, both $\bar{u}$ and $\bar{w}$ should be null vectors, a fact that can be achieved by ensuring that $\alpha_i = 0,\ i = 1, 2, 3$.

The approximation (1) can be specified for a given node k, according to:

$$\bar{u}_k = \bar{u}\left[X_k^*, \underbrace{\frac{\left(X_k^* - O\right).N}{\left|\left(X_k^* - O\right).N\right|}}_{r}\right] \tag{3}$$

in $\Omega_1 \cup \Omega_2$.

A notation for the scalar components of $\bar{u}_k$ can be carried out as: $\bar{u}_{k1} = f_{k1}(\alpha_1, \alpha_2, \alpha_3)$ and $\bar{u}_{k2} = f_{k2}(\alpha_1, \alpha_2, \alpha_3)$.

With the introduction of the particular case (3), it is possible to define the contribution of the crack to the rigid body displacement field as:

$$\bar{u} = H_k \bar{u}_k \tag{4}$$

in which H_k are the standard isoparametric shape functions for the quadrilateral.

The total displacement field, $\boldsymbol{u}$, can then be determined as the sum of the regular displacement (which is identified with a hat, $\hat{u}$) and the jump:

$$u = \underbrace{\hat{u}}_{regular} - \underbrace{\bar{u}}_{jump} \tag{5}$$

The regular displacement field corresponds to the displacement that occurs in the element represented in grey in Figure 1, but without considering the discontinuity.

2.3 The deformation gradient and the spatial velocity gradient

With the definition of the displacement increment field, and hence of the displacement field, the derived quantities follow using classical relations from continuum mechanics (see the presentation given by Haupt [4]).

The discretized form of the deformation gradient can be written as:

$$F = \hat{F} - \bar{F} + I + \delta_\Gamma \bar{w} \otimes N \qquad in\ \ \Omega \tag{6}$$

The term δ_Γ in equation (6) represents the Dirac delta function defined on the set Γ. The terms $\hat{F}$ and $\bar{F}$ can be evaluated according to its scalar components:

$$\hat{F}_{ij} = \frac{\partial H_k}{\partial X_j}\left(X_{ki} + u_{ki}\right) \qquad in\ \ \Omega_1 \cup \Omega_2 \tag{7}$$

and

$$\bar{F}_{ij} = \frac{\partial H_k}{\partial X_j}\left(X_{ki} + \bar{u}_{ki}\right) \qquad in\ \Omega_1 \cup \Omega_2 \tag{8}$$

The spatial velocity gradient (in Ω) can be denoted as $\boldsymbol{L}$, and its scalar components are:

$$L_{ij} = \frac{\partial H_k}{\partial x_j}\dot{u}_{ki} + g_{ijp}\dot{\alpha}_p + \delta_\Gamma \dot{\bar{w}}_i N_k F_{kj}^{-1} \quad in\ \ \Omega \tag{9}$$

In equation (9), the quantity

$$g_{ijp} = -\frac{\partial H_r}{\partial x_j}\frac{\partial f_r}{\partial \alpha_p} \tag{10}$$

was introduced.

2.4 Existence of the displacement discontinuity

If the displacement discontinuity does not exist, which occurs when a fracture criterion is not satisfied, then $\alpha_i = 0$. This is imposed through the introduction of a function h of the crack state which is defined as:

$$h = \begin{cases} 0 & crack\ closed \\ 1 & crack\ opened \end{cases}$$

If h= 0 then $\alpha_i = 0$ for $i = 1, 2, 3$. A suitable method for imposing the constraints $\alpha_i = 0$ is the Lagrange multiplier method, which is here adopted.

3 Equilibrium equations and related discretized forms

Let V_0 represent the material integration volume corresponding to the domain $\Omega_1 \cup \Omega_2$ and v_0 represent the spatial integration volume corresponding to the same domain. The element is defined as Ω.

The crack zone itself is represented by the material integration line l_0. A given point $X \in \Omega_1 \cup \Omega_2$ is represented by its material coordinates $\boldsymbol{X}$ and spatial coordinates $\boldsymbol{x}$=$\boldsymbol{X}$+$\boldsymbol{u}$.

As $\bar{u}(\boldsymbol{X})$ and $\hat{u}(\boldsymbol{X})$ are two independent fields, they can be used to introduce kinematically admissible virtual displacements $\delta\,\bar{u}$ and $\delta\,\hat{u}$ to project the equilibrium equations and obtain a weak form.

The existence of a volume force field represented by its material vector $b\,(X)$ is assumed.

If $\tau\,(F)$ represents the Kirchhoff stress tensor, then the weak form of equilibrium can be exposed as:

$$\int_{Vo} \tau\,(F) : \nabla_x\,\delta u\ dVo + \int_{lo} \delta\bar{w}\,.\,t\ dlo = \int_{Vo} b\,.\,\delta u\ dVo \quad in\ \Omega \tag{11}$$

This project form is very similar to the standard projected form for a non-cracked element (with the noticeable exception of the crack term).

The condition for the non-existence of the crack is introduced imposing $\bar{u}_i = 0$ for $h = 0$. Additionally, the condition for crack closure should be introduced for $h = 1$. If Lagrange multipliers λ are introduced then:

$$\int_{Vo} \tau\left(F\right) : \nabla_x \delta u \; dVo + \int_{lo} \delta \bar{w} \, . t \; dlo + \; \delta \left[\lambda \left(\left(1-h\right)\alpha + h\,\lambda\right)\right] = \int_{Vo} b \, . \, \delta u \; dVo \tag{12}$$

For the application of the Newton-Raphson method, the first variations of equation (12) are required.

4 Particular constitutive relations for the discrete crack

4.1 Fracture criterion

If the crack has not initiated yet, which occurs for the indicator $h = 0$, the following criterion for the crack initiation is adopted for a given element:

$$\breve{\tau}_1 \geq \tau_{1c} \tag{13}$$

where τ_{1c} is the maximum allowable positive Kirchhoff principal stress and $\bar{\tau}_{1c}$ is the following quantity:

$$\breve{\tau}_1 = \frac{1}{Vo} \int_{Vo} \max\left(0, \tau_1\right) dVo \tag{14}$$

with τ_1 being the maximum principal Kirchhoff stress.

The definition of h is carried out using the maximum value of $\bar{\tau}_{1c}$ during the deformation history:

$$h = H\left[\underbrace{\max}_{history}\left(\breve{\tau}_1\right) - \tau_{1c}\right] \tag{15}$$

The function H in definition (15) is the unit step function. The calculation of the natural coordinates ξ_Q of a point Q located on the crack is carried out using the following relation where ξ_X represent the natural coordinates of a point $X \in \Omega_1 \cup \Omega_2$:

$$\xi_Q = \frac{\int_{Vo} \max\left(0, \tau_1\right) \; \xi_X \; dVo}{Vo \;\; \breve{\tau}_1} \tag{16}$$

The calculation of the material coordinates of the normal vector, $\boldsymbol{N}$, is accomplish according to:

$$\mathbf{N} = \frac{\int_{Vo} \max\left(0, \tau_1\right) \; \mathbf{N_1} \; dVo}{Vo \;\; \breve{\tau}_1} \tag{17}$$

where $\boldsymbol{N}_1$ is the second Piola-Kirchhoff stress principal direction.

4.2 Interface compliance

The calculate $\boldsymbol{t}$ as a function of $\boldsymbol{w}$, the local spatial coordinates of $\boldsymbol{t}$ in the frame $\{\boldsymbol{s},\boldsymbol{n}\}$ are introduced:

$$t_1 = \mathbf{t}.\mathbf{s} \tag{18a}$$

$$t_2 = \mathbf{t}.\mathbf{n} \tag{18b}$$

Introducing an internal kinematic variable, k, the following local constitutive law is assumed for t_1 and t_2:

$$\left\{ \begin{array}{c} t_1 \\ t_2 \end{array} \right\} = \left\{ \begin{array}{cc} d_{int} & w_1 \\ \left[\Xi\left(k\right) & H\left(w_2\right) + \rho\, H\left(-w_2\right)\right] \quad w_2 \end{array} \right\} \tag{19}$$

where $\Xi\left(k\right)$ is the following function of k:

$$\Xi\left(k\right) = \frac{\tau_{1c}}{k}\, \exp\left(-\frac{\tau_{1c}}{G_f} k\right) \tag{20}$$

and ρ is a penalty parameter.

The value of ρ is taken as the absolute value of the interface compliance before initiation:

$$\rho = \frac{\tau_{1c}^2}{G_f} = -\lim_{w_2 \to 0^+} \frac{\partial t_2}{\partial w_2} \tag{21}$$

In equation (20) the term G_f represents the fracture energy, the term k is calculated using the historical evaluation of w_2:

$$k = \max_{history} \left[\max\left(0, w_2\right)\right] \tag{22}$$

The property d_{int} in equation (19) is the shear stiffness of the crack. A constant value of d_{int} is here adopted, but distinct strategies are possible (see reference [9]).

5 Numerical integration

For the domain $\Omega_1 \cup \Omega_2$, a standard Gaussian quadrature is adopted. For the crack, a nodal integration rule is employed. Due to the definition of the crack position, both Ω_1 and Ω_2 contain at least one Gauss point.

The integration points are presented in Figure 2.

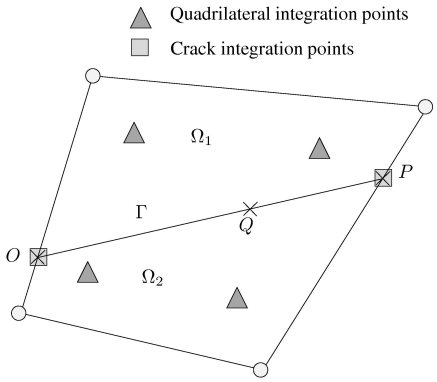

Figure 2: The integration points in the crack and in the quadrilateral.

6 Numerical examples

6.1 Three point bending: mode I small strain test

This test consists in the bending of a cracked beam. A pre-existent crack is located at the mid span and propagates upwards as the loading increases. Figure 3 shows the geometry, boundary conditions and material properties of the model.

The geometrical data and the boundary conditions are taken form references [1, 3].

Two mesh densities are used, with the purposed of inspecting some possible mesh size dependency of the crack propagation. The deformed meshes for 2 mm mid span displacement (scaled $100\times$) are represented in Figure 4. The sparse mesh contains 1268 elements and the refined mesh contains 2099 elements.

The force magnitude is plotted as a function of the mid-span transversal displacement in Figure 5. Along with the results obtained with the proposed formulation, some experimental values, which were obtained by Peterson (see reference [1] for further details) are also presented. There is a very close agreement between the numerical results and the experimental ones. For comparison, the use of a gradient regularized media (see reference [3]) is not sufficient to represent the experimental results.

6.2 Debounding problem: a finite strain test

This test consists on the finite strain analysis of a debounding problem.

The purpose of this analysis is to separate two initially bonded plates by pulling the top notch. This test was carried out by Oliver *et al.* with triangular elements (see reference [7]) and a very refined mesh.

Four distinct steps of the debounding analysis are represented in figure 6, where the contour plot of the horizontal Kirchhoff stress τ_{11} is also represented. The crack tip can be identified by

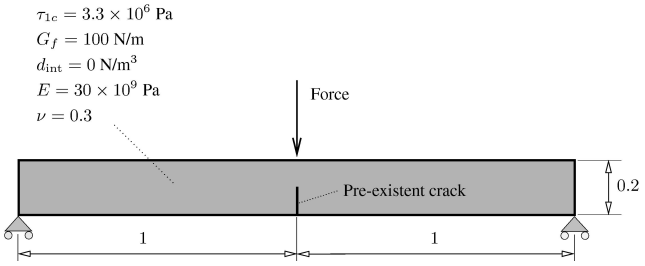

Figure 3: Three point bending of a cracked beam (all dimensions are in mm).

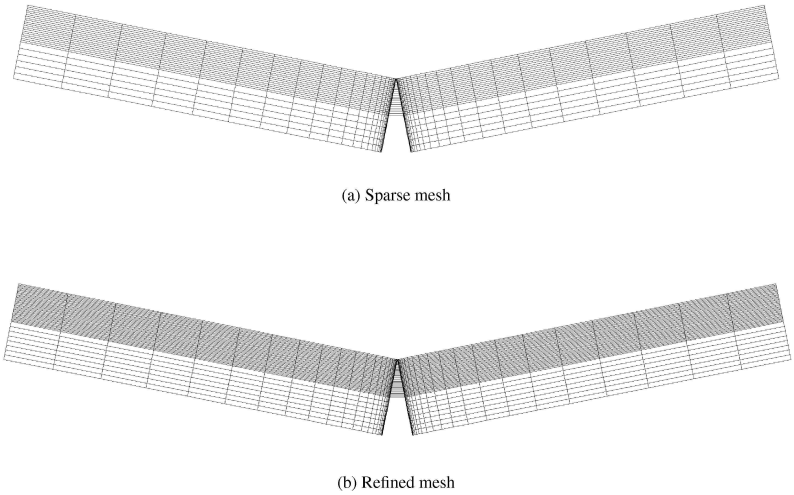

Figure 4: The deformed meshes (with a scale factor of 100) corresponding to two distinct mesh densities.

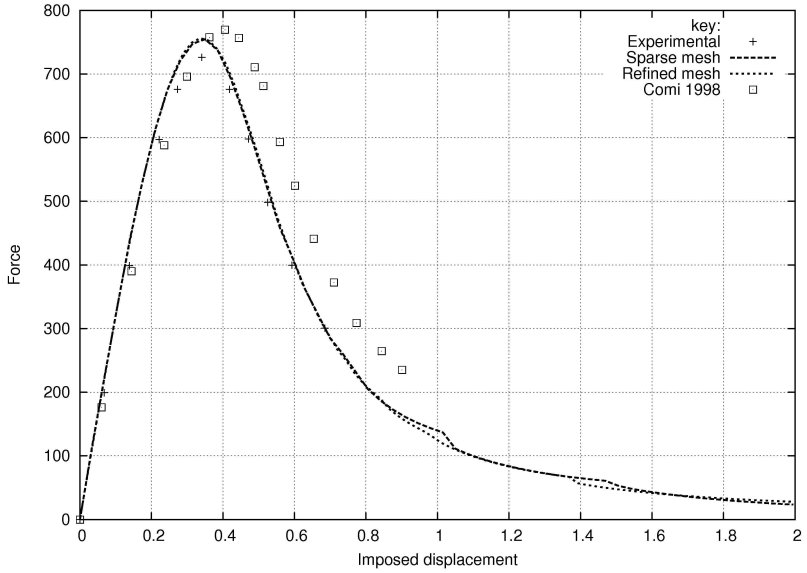

Figure 5: The force-displacement plot for the three point bending test (see Figure 3). The experimental points were produced from reference [1].

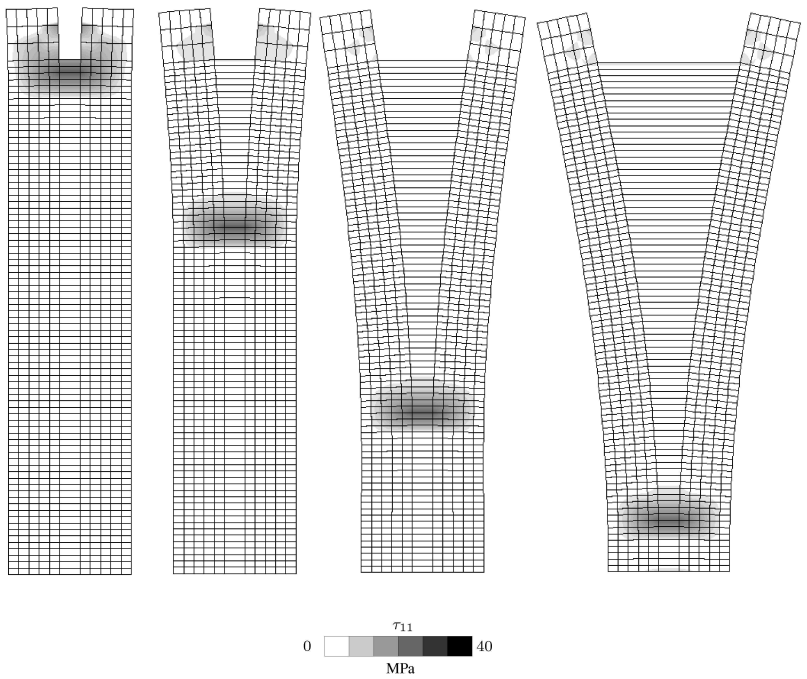

Figure 6: Four distinct steps in the analysis of the debounding problem. The τ_{11} stress component contour plot is also presented.

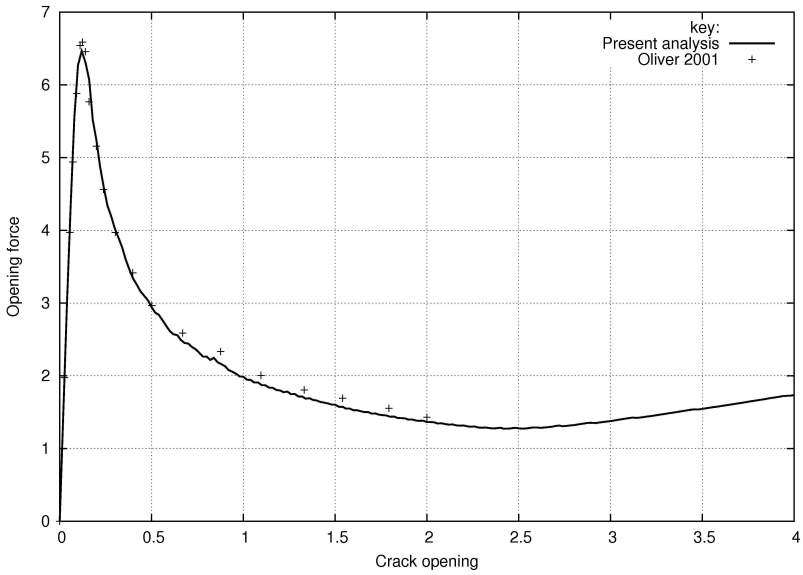

Figure 7: Force-crack opening plot for the debounding problem. Comparison with reference [7].

the very high stress gradient.

Finally, the force-crack opening is presented in Figure 7 and is compared with the results from reference [7].

7 Conclusions

The proposed formulation allows accurate results (at least in mode I) for brittle fracture, as was observed.

The robustness is very high, which is a consequence of the exact linearization and also of the symmetric and isoparametric treatment of the rigid body motion induced by the crack. Further developments are being carried out to accurately model mixed mode fracture and finite strain plasticity.

References

[1] J. Alfaiate, A. Simone, and L. J. Sluys. A new approach to strong embedded discontinuities. In N. Bicanic, R. de Borst, H. Mang, and G. Meschke, editors, *Computational modelling of Concrete Structures, EURO-C 2003*, Salzburger Land, Austria, March 2003. St. Johann im Pongau.

[2] J. Alfaiate, G. N. Wells, and L. J. Sluys. On the use of embedded discontinuity elements with crack path continuity for mode-I and mixed-mode fracture. *Engineering Fracture Mechanics*, 69:661–686, 2002.

[3] Comi and L. Driemeier. *Material Instabilities in Solids, chapter 26.* John Wiley and Sons, 1998.

[4] P. Haupt. *Continuum Mechanics and Theory of Materials, second edition.* Springer-Verlag, 2002.

[5] M. Jirasek and T. Zimmermann. Embedded crack model. I: Basic formulation. *International Journal for Numerical Methods in Engineering*, 50:1269–1290, 2001.

[6] M. Jirasek and T. Zimmermann. Embedded crack model. II: Combination with smeared cracks. *International Journal for Numerical Methods in Engineering*, 50:1291–1305, 2001.

[7] J. Oliver, A. Huespe, D. Pulido, and E. Samaniego. On strong discontinuity approach in finite deformation settings. In *Monograph CIMNE 62, International Center for Numerical Methods in Engineering*, Barcelona, Spain,, October 2001.

[8] L. J. Sluys and A. H. Berends. Discontinuous failure analysis for mode-I and mode-II localization problems. *International Journal of Solids and Structure*, 35:4257–4274, 1998.

[9] G. N. Wells and L. J. Sluys. A new method for modelling cohesive cracks using finite elements. *International Journal for Numerical Methods in Engineering*, 50:2667–2682, 2001.